ACADEMIC PRESS

Available online at www.sciencedirect.com

SCIENCE DIRECT®

Journal of Sound and Vibration 262 (2003) 65–86

JOURNAL OF SOUND AND VIBRATION

www.elsevier.com/locate/jsvi

Vibration analysis of laminated cross-ply oval cylindrical shells

M. Ganapathi, B.P. Patel*, H.G. Patel, D.S. Pawargi

Institute of Armament Technology, GM Faculty, Girinager, Pune 411 025, India

Received 4 February 2002; accepted 18 June 2002

Abstract

Here, free vibrations and transient dynamic response analyses of laminated cross-ply oval cylindrical shells are carried out. The formulation is based on higher order theory that accounts for the transverse shear and the transverse normal deformations, and includes zig-zag variation in the in-plane displacements across the thickness of the multi-layered shells. The contributions of inertia effect due to in-plane and rotary motions, and the higher order function arising from the assumed displacement models are included. The governing equations obtained using Lagrangian equations of motion are solved through finite element approach. A detailed parametric study is conducted to bring out the influence of different shell geometry, ovality parameter, lay-up and loading environment on the vibration characteristics related to different modes of vibrations of oval shell.

1. Introduction

Laminated composite cylinders are increasingly used as load-carrying elements in modern engineering systems. This is especially true of the aerospace, nuclear, marine, petrochemical, biomedical and construction industries, where dramatic and sophisticated uses are currently being made of shells in flight vehicles, nuclear reactor vessels, deep submersibles, refinery and biomedical equipment, and roofs for industrial buildings. Furthermore, fiber-reinforced composites provide high specific strength and stiffness, as well as the ability to tailor these parameters for achieving minimal weight. Although circular cylindrical shell is a simple structural component, the cross-section of such cylinders may become non-circular either due to the fabrication process or due to the design considerations, for example, non-circular structural components in aerospace and submersible systems. This may lead to the increase in the level of geometrical complexities. The analysis of such cylinders is important because the out of roundness

*Corresponding author. Tel.: +91-020-599-550; fax: +91-020-599-509.
E-mail address: badripatel@hotmail.com (B.P. Patel).

0022-460X/03/$ - see front matter
PII: S0022-460X(02)01025-8

may adversely affect the vibration characteristics. Thus, studies concerning composite non-circular cylindrical shells have gained importance recently in the literature.

The vibration analysis of shells of revolution has received considerable attention in the literature and has been reviewed by Leissa [1], Noor [2], Noor and Burton [3], Qatu [4] and Soldatos [5]. Recently, the study pertaining to non-circular cylindrical shells has been reviewed and well documented by Soldatos [6]. It can be concluded that the number of studies that deal with the dynamic characteristics of non-circular shells is rather limited, and it is due to the difficulty introduced in governing equations because of the cross-sectional radius of curvature as a function of an arc co-ordinate. It can be further opined from the literature that few contributions are available concerning with the free vibration analysis of anisotropic laminated non-circular cylindrical shells compared to those of isotropic case and they are cited here. Using the classical theory, Soldatos and Tzivanidis [7], Soldatos [8], Hui and Du [9], and Suzuki et al. [10] have studied the vibration characteristics of thin laminated non-circular shells through analytical methods. Donnell- and Flugge-type shell theories have been employed in the work of Soldatos and Tzivanidis [7] and Soldatos [8], respectively, and the solutions are obtained using the method of Galerkin. Hui and Du [9] have analyzed the effect of geometric imperfection on non-circular shells by introducing Donnell-type shell theory and adopting Galerkin's method for solving the governing equations. Suzuki et al. [10] have applied Love-type shell theory in conjunction with power method. Noor [11], Kumar and Singh [12], and Suzuki et al. [13] have introduced first order shear deformation theory (FSDT) for analyzing such structures. Noor [11] has solved the problem using Sanders–Koiter shell theory and multilocal difference discretization method, while Kumar and Singh [12] have employed Bezier functions technique to Love-type shell theory. Suzuki et al. [13] have obtained the solutions using power method. The study employing parabolic shear deformation theory is attempted for isotropic case in the work of Soldatos [14]. However, the analyses concerning forced vibrations of non-circular laminated cylindrical shells seem to be scarce in the literature, except the work of Cheung [15] that is concerned with thin isotropic shells based on Donnell-type classical theory in conjunction with the finite strip method.

It is evident from the literature that first order theory can predict fairly accurate results for the estimation of global behaviors of laminates like deflection, fundamental frequency and buckling load, etc. However, it is inadequate for the accurate estimation of higher order frequencies, mode shapes, large deflections and distribution of stresses. This has necessitated the introduction of higher order function in the displacement model and layerwise theory for the study of laminated plates and circular cylindrical shells [16–22]. To the authors' knowledge, the studies based on higher order models appear to be scarce in the literature for the analysis of non-circular cylindrical shells.

In the present work, the free vibration characteristics, and forced vibration responses of oval cylindrical shells subjected to thermal/mechanical loads based on finite element procedure are studied by extending the higher order displacement model including zig-zag theory and the variable transverse displacement through the thickness [23,24]. The formulation includes all the inertia terms, due to the parts resulting from the first order model, the higher order displacement function, and the coupling between the different order displacements. The accuracy of the present model is tested against the available analytical/numerical solutions. A detailed parametric study is carried out to highlight the influence of non-circularity/ovality parameter, thickness and

slenderness ratios and lay-up on the natural frequencies, and forced vibration characteristics of laminated composite oval shells.

2. Formulation

A laminated composite non-circular cylindrical shell is considered with the co-ordinates x along the meridional direction, y along the circumferential direction and z along the thickness direction having origin at the mid-plane of the shell as shown in Fig. 1. Based on Taylor's series expansion method for deducing the two-dimensional formulation of a three-dimensional elasticity problem, the in-plane displacements u^k and v^k, and the transverse displacement w^k for the kth layer, are assumed as (a list of nomenclature is given in Appendix B).

$$u^k(x,y,z,t) = u_0(x,y,t) + z\theta_x(x,y,t) + z^2\beta_x(x,y,t) + z^3\phi_x(x,y,t) + S^k\psi_x(x,y,t),$$
$$v^k(x,y,z,t) = v_0(x,y,t) + z\theta_y(x,y,t) + z^2\beta_y(x,y,t) + z^3\phi_y(x,y,t) + S^k\psi_y(x,y,t),$$
$$w^k(x,y,z,t) = w_0(x,y,t) + zw_1(x,y,t) + z^2\Gamma(x,y,t). \tag{1}$$

Here, u_0, v_0, w_0 are the displacements of a generic point on the reference surface; θ_x, θ_y are the rotations of normal to the reference surface about the y- and x-axis, respectively; w_1, β_x, β_y, Γ, ϕ_x, ϕ_y are the higher order terms in the Taylor's series expansions, defined at the reference surface. ψ_x and ψ_y are the generalized variables associated with the zig-zag function, S^k.

The zig-zag function, S^k, as given in the work of Murakami [25], is defined by

$$S^k = 2(-1)^k z_k/t_k, \tag{2}$$

where z_k is the local transverse co-ordinate with its origin at the center of the kth layer and t_k is the corresponding layer thickness. Thus, the zig-zag function is piecewise linear with values of -1

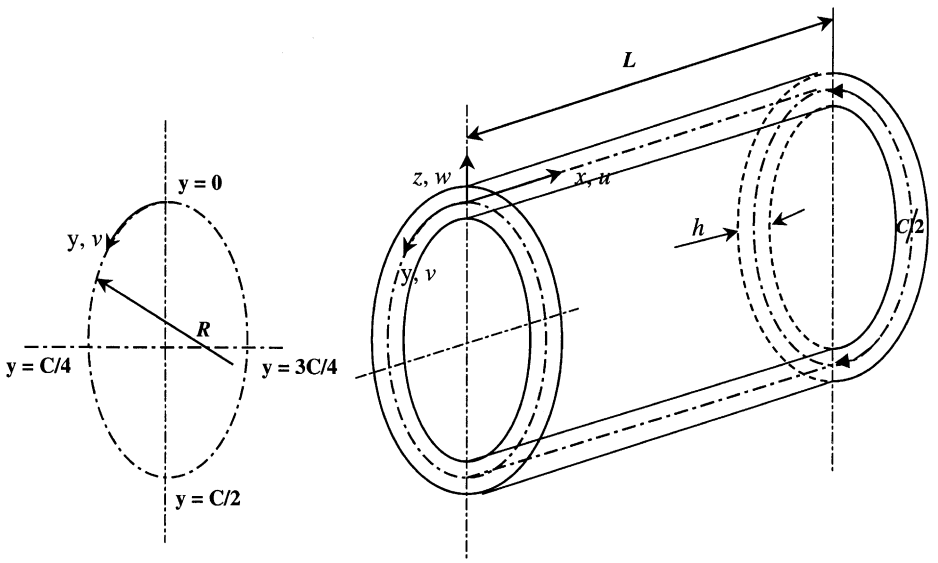

Fig. 1. Generalized co-ordinate system and cross-sectional details of the oval shell.

and 1 alternately at the different interfaces. The 'zig-zag' function, as defined above, takes care of the inclusion of the slope discontinuity of u and v at the interfaces of the laminate as observed in exact three-dimensional elasticity solutions of thick laminated composite structures. The use of such function is more economical than a discrete layer approach of approximating the displacement variations over the thickness of each layer separately. Although both these approaches account for slope discontinuity at the interfaces, in the discrete layer approach the number of unknowns increases with the increase in the number of layers, whereas it remains constant in the present approach.

The strains in terms of mid-plane deformation, rotations of normal, and higher order terms associated with displacements for kth layer are as

$$\{\varepsilon\} = \begin{Bmatrix} \varepsilon_{bm} \\ \varepsilon_s \end{Bmatrix} - \begin{Bmatrix} \bar{\varepsilon}_t \\ 0 \end{Bmatrix}. \tag{3}$$

The vector $\{\varepsilon_{bm}\}$ includes the bending and membrane terms of the strain components and vector $\{\varepsilon_s\}$ contains the transverse shear strain terms. These strain vectors can be defined as

$$\begin{Bmatrix} \varepsilon_{bm} \\ \varepsilon_S \end{Bmatrix} = \begin{Bmatrix} \varepsilon_{xx} \\ \varepsilon_{yy} \\ \varepsilon_{zz} \\ \gamma_{xy} \\ \gamma_{xz} \\ \gamma_{yz} \end{Bmatrix} = \begin{Bmatrix} u^k_{,x} \\ (v^k_{,y} + w^k/R)/(1 + z/R) \\ w^k_{,z} \\ u^k_{,y}/(1 + z/R) + v^k_{,x} \\ u^k_{,z} + w^k_{,x} \\ v^k_{,z} + (w^k_{,y} - v^k/R)/(1 + z/R) \end{Bmatrix}, \tag{4a}$$

where R, the principal radii of curvature in the circumferential direction, is the function of circumferential co-ordinate y. The variation of R in the circumferential direction depends on the type of cross-section, i.e., for instance, for oval cross-section, the variable curvature R can be described as

$$R_o/R = 1 + \xi \cos(2y/R_o), \quad (0 \leqslant \xi \leqslant 1), \tag{4b}$$

where ξ and y are non-circularity/ovality parameter and the circumferential cordinate, respectively. R_o is the average radius of curvature of the middle surface and is equal to $C/2\pi$; C is the total circumferential length of the oval shell.

Using the kinematics given in Eq. (1), Eq. (4a) can be rewritten as

$$\begin{Bmatrix} \varepsilon_{bm} \\ \varepsilon_s \end{Bmatrix} = [\bar{Z}]\{\ \varepsilon_1 \quad \varepsilon_2 \quad \varepsilon_3 \quad \varepsilon_4 \quad \varepsilon_5 \quad \varepsilon_6 \quad \varepsilon_7 \quad \varepsilon_8 \quad \varepsilon_9 \quad \varepsilon_{10}\ \}^{\mathrm{T}}, \tag{5a}$$

where

$$[\bar{Z}] = \begin{bmatrix} Z_1 & Z_2 & Z_3 & Z_4 & Z_5 & O_1 & O_1 & O_1 & O_1 & O_2 \\ O_1^{\mathrm{T}} & O_1^{\mathrm{T}} & O_1^{\mathrm{T}} & O_1^{\mathrm{T}} & O_2^{\mathrm{T}} & Z_6 & Z_7 & Z_8 & Z_9 & Z_{10} \end{bmatrix}. \tag{5b}$$

The various submatrices involved in Eq. (5) are given in Appendix A.

The subscript comma denotes the partial derivative with respect to the spatial co-ordinate succeeding it.

The thermal strain vector $\{\bar{\varepsilon}_t\}$ is represented as

$$\{\bar{\varepsilon}_t\} = \begin{Bmatrix} \bar{\varepsilon}_{xx} \\ \bar{\varepsilon}_{yy} \\ \bar{\varepsilon}_{zz} \\ \bar{\varepsilon}_{xy} \\ \bar{\varepsilon}_{xz} \\ \bar{\varepsilon}_{yz} \end{Bmatrix} = \Delta T \begin{Bmatrix} \alpha_x \\ \alpha_y \\ \alpha_z \\ \alpha_{xy} \\ 0 \\ 0 \end{Bmatrix}, \tag{5c}$$

where ΔT is the rise in temperature and is generally represented as the function of x, y and z. α_x, α_y, α_z and α_{xy} are thermal expansion coefficients in the shell co-ordinates and can be related to the thermal coefficients (α_1, α_2 and α_3) in the material principal directions.

The constitutive relations for an arbitary layer k, in the laminated shell (x, y, z) co-ordinate system can be expressed as

$$\begin{aligned} \{\sigma\} &= \{\, \sigma_{xx} \quad \sigma_{yy} \quad \sigma_{zz} \quad \tau_{xy} \quad \tau_{xz} \quad \tau_{yz} \,\}^{\mathrm{T}} \\ &= [\bar{Q}_k]\{\, \varepsilon_{xx} - \bar{\varepsilon}_{xx} \quad \varepsilon_{yy} - \bar{\varepsilon}_{yy} \quad \varepsilon_{zz} - \bar{\varepsilon}_{zz} \quad \gamma_{xy} - \bar{\gamma}_{xy} \quad \gamma_{xz} \quad \gamma_{yz} \,\}^{\mathrm{T}}, \end{aligned} \tag{6}$$

where the terms of $[\bar{Q}_k]$ matrix of kth ply are referred to the laminated shell axes and can be obtained from the $[Q_k]$ corresponding to the fiber directions with the appropriate transformation, as outlined in the literature [26]. $\{\sigma\}$, $\{\varepsilon\}$ and $\{\bar{\varepsilon}_t\}$ are stress, strain, and thermal strain vectors due to rise in temperature, respectively. The superscript T refers to transpose of a matrix/vector.

The governing equations are obtained by applying Lagrangian equations of motion given by

$$\mathrm{d}/\mathrm{d}t[\partial(T - U_T)/\partial\dot{\delta}_i] - [\partial(T - U_T)/\partial\delta_i] = 0, \quad i = 1 \text{ to } n, \tag{7}$$

where T is the kinetic energy; U_T is the total potential energy consisting of strain energy contributions due to the in-plane and transverse stresses, and work done by the externally applied mechanical loads, respectively. $\{\delta\} = \{\delta_1, \delta_2, \ldots, \delta_i, \ldots, \delta_n\}^{\mathrm{T}}$ is the vector of the degrees of freedom/generalized co-ordinates. A dot over the variables represents the partial derivative with respect to time.

The kinetic energy of the plate is given by

$$T(\dot{\delta}) = \frac{1}{2}\int\int \sum_{k=1}^{N} \int_{h_k}^{h_{k+1}} \rho_k \int \{\, \dot{u}^k \quad \dot{v}^k \quad \dot{w}^k \,\}\{\, \dot{u}^k \quad \dot{v}^k \quad \dot{w}^k \,\}^{\mathrm{T}} \left(1 + \frac{z}{R}\right) \mathrm{d}z]\, \mathrm{d}x\, \mathrm{d}y, \tag{8}$$

where ρ_k is the mass density of the kth layer. h_k, h_{k+1} are the z co-ordinates of laminate corresponding to the bottom and top surfaces of the kth layer.

Using the kinematics given in Eq. (1), Eq. (8) can be rewritten as

$$T(\dot{\delta}) = \frac{1}{2}\int\int \sum_{k=1}^{N} \int_{h_k}^{h_{k+1}} \rho_k \{\dot{d}^e\}^{\mathrm{T}}[Z]^{\mathrm{T}}[Z]\{\dot{d}^e\} \left(1 + \frac{z}{R}\right) \mathrm{d}z]\, \mathrm{d}x\, \mathrm{d}y, \tag{9}$$

where $\{\dot{d}^e\}^{\mathrm{T}} = \{\dot{u}_0 \quad \dot{v}_0 \quad \dot{w}_0 \quad \dot{\theta}_x \quad \dot{\theta}_y \quad \dot{w}_1 \quad \dot{\beta}_x \quad \dot{\beta}_y \quad \dot{\Gamma} \quad \dot{\phi}_x \quad \dot{\phi}_y \quad \dot{\psi}_x \quad \dot{\psi}_y\}$ and

$$[Z] = \begin{bmatrix} 1 & 0 & 0 & z & 0 & 0 & z^2 & 0 & 0 & z^3 & 0 & S^k & 0 \\ 0 & 1 & 0 & 0 & z & 0 & 0 & z^2 & 0 & 0 & z^3 & 0 & S^k \\ 0 & 0 & 1 & 0 & 0 & z & 0 & 0 & z^2 & 0 & 0 & 0 & 0 \end{bmatrix}.$$

The potential energy functional U_T is given by

$$U_T(\delta) = \frac{1}{2}\int\int\left[\sum_{k=1}^{N}\int_{h_k}^{h_{k+1}}\{\sigma\}^{\mathrm{T}}\varepsilon\left(1+\frac{z}{R}\right)\mathrm{d}z\right]\mathrm{d}x\,\mathrm{d}y - \int\int qw\,\mathrm{d}x\,\mathrm{d}y, \tag{10}$$

where q is the distributed force acting on the bottom surface of the shell.

For obtaining the element level governing equations, the kinetic and the total potential energies may be conveniently written as

$$T(\delta^e) = \tfrac{1}{2}\{\dot{\delta}^e\}^{\mathrm{T}}[M^e]\{\dot{\delta}^e\}, \tag{11}$$

$$U_T(\delta^e) = \tfrac{1}{2}\{\delta^e\}^{\mathrm{T}}[K^e]\{\delta^e\} - \{\delta^e\}^{\mathrm{T}}\{F_T^e\} - \{\delta^e\}^{\mathrm{T}}\{F_M^e\} + \frac{1}{2}\int\int\left[\sum_{k=1}^{N}\int_{h_k}^{h_{k+1}}\{\bar{\varepsilon}_t\}^{\mathrm{T}}[\bar{Q}]\{\bar{\varepsilon}_t\}\left(1+\frac{z}{R}\right)\mathrm{d}z\right]\mathrm{d}x\,\mathrm{d}y. \tag{12}$$

The elemental mass and stiffness matrices, and thermal/mechanical load vectors involved in Eqs. (11) and (12) can be defined as

$$[M^e] = \int\int\left[\sum_{k=1}^{N}\int_{h_k}^{h_{k+1}}\rho_k\{H\}^{\mathrm{T}}[Z]^{\mathrm{T}}[Z]\{H\}\left(1+\frac{z}{R}\right)\mathrm{d}z\right]\mathrm{d}x\,\mathrm{d}y, \tag{13}$$

$$[K^e] = \int\int\left[\sum_{k=1}^{N}\int_{h_k}^{h_{k+1}}[B]^{\mathrm{T}}\left[\bar{Z}\right]^{\mathrm{T}}\left[\bar{Q}_k\right]\left[\bar{Z}\right][B]\left(1+\frac{z}{R}\right)\mathrm{d}z\right]\mathrm{d}x\,\mathrm{d}y, \tag{14}$$

$$\{F_T^e\} = \int\int\left[\sum_{k=1}^{N}\int_{h_k}^{h_{k+1}}[B]^{\mathrm{T}}\left[\bar{Z}\right]^{\mathrm{T}}\left[\bar{Q}_k\right]\{\bar{\varepsilon}_t\}\left(1+\frac{z}{R}\right)\mathrm{d}z\right]\mathrm{d}x\,\mathrm{d}y,$$

and

$$\{F_M^e\} = \int\int\{H_w\}^{\mathrm{T}}q\,\mathrm{d}x\,\mathrm{d}y. \tag{15}$$

Here $\{\delta^e\}$ is the vector of the elemental degrees of freedom/generalized co-ordinates, and $[H]$ and $[B]$ are the interpolation and strain matrices pertaining to the element, respectively.

Substituting Eqs. (11) and (12) in Eq. (7), one obtains the governing equation for the element as

$$[M^e]\{\ddot{\delta}^e\} + [K^e]\{\delta^e\} = \{F_T^e\} + \{F_M^e\}. \tag{16}$$

The coefficients of mass and stiffness matrices, and the load vectors involved in governing Eq. (16) can be rewritten as the product of term having thickness co-ordinate z alone and the term containing x and y. In the present study, while performing the integration, terms having thickness co-ordinate z are explicitly integrated, whereas the terms containing x and y are evaluated using full integration with 5×5 points Gauss integration rule.

Following the usual finite element assembly procedure [27], the governing equation for the forced/free response of the laminated shell are obtained as

$$[M]\{\ddot{\delta}\} + [K]\{\delta\} = \{F_T\} + \{F_M\} \quad \text{(Forced vibration)}, \tag{17a}$$

$$[M]\{\ddot{\delta}\} + [K]\{\delta\} = \{0\} \quad \text{(Free vibration)}, \tag{17b}$$

where $[M]$ and $[K]$ are the global mass and stiffness matrices. $\{F_T\}$ and $\{F_M\}$ are the global thermal and mechanical load vectors, repectively.

The solutions of Eqs. (17a) and (17b) can be obtained using Newmark's direct time integration method and standard eigenvalue extraction procedures, respectively.

3. Element description

In the present work, a simple C^0 continous, eight-noded serendipity quadrilateral shear flexible shell element (HSDT) with 13 nodal degrees of freedom (u_0, v_0, w_0, θ_x, θ_y, w_1, β_x, β_y, Γ, ϕ_x, ϕ_y, ψ_x and ψ_y: 13 d.o.f.) developed based on field consistency approach [28] is employed.

If the interpolation functions for an eight-noded element are used directly to interpolate the 13 field variables $u_0, \ldots, \psi_y$ in deriving the membrane and shear strains, the element will lock and show oscillation in the membrane and shear stresses. Field consistency requires that the membrane and the transverse shear strains must be interpolated in a consistent manner, as outlined in Ref. [28]. This is achieved here by smoothing the original interpolation functions in a least-squares accurate fashion to the desired form, i.e., the functions that are consistent with the derivative functions. Here, we need smoothed functions for w_0 term and the terms (θ_x and θ_y) which are consistent with the interpolations for $v_{0,y}$; and ($w_{0,x}$ and $w_{0,y}$) to substitute in the membrane strain expression $\{\varepsilon_1\}$ given in Eq. (A.2), and in the transverse shear strain definition $\{\varepsilon_6\}$ given in Eq. (A.3), respectively. It can be noted that $v_{0,y}$; and ($w_{0,x}$ and $w_{0,y}$) are of the quadratic form in x and y, respectively, as the original interpolation function for any field variable is of cubic type for the eight-noded element chosen here. This means that the smoothed functions that must be derived for w_0 term and the terms (θ_x and θ_y) by smoothing the original interpolation function, be consistent with the derivative functions, $v_{0,y}$; and ($w_{0,x}$ and $w_{0,y}$), respectively. The element thus derived is tested for its basic properties and is found free from the rank deficiency, shear/membrane locking, and poor convergence syndrome [29].

4. Results and discussion

The analysis, here, is concerned with the free vibration characteristics and transient dynamic responses of simply supported oval cross-ply cylindrical shells. Since the higher order theory, in general, is required for the accurate analysis of thick composite structures, the emphasis in the present work is placed on the laminated shells with thickness ratios $R_o/h \leqslant 20$. As the element employed here is based on the field consistent approach, all the strain energy terms are calculated using exact numerical integration scheme. The influence of various parameters such as thickness and length ratios (R_o/h and L/R_o), ovality parameter (ξ) and number of layers (N) on the

non-dimensional natural frequencies corresponding to various nominal circumferential wave numbers $\bar{n}$ (defined based on the criterion suggested in Ref. [30]) corresponding to different types of vibration modes of shells is examined. It can be noted here that unlike the circular case, the conventional manner of describing the mode based on number of crossings is not actually valid as the effect of variable curvature of oval shell introduces coupling of the circumferential modes corresponding to circular one. This was the reason why nominal circumferential wave numbers $\bar{n}$ has been introduced. The in-plane and transverse response behaviors of the oval shells under different loads are also investigated. Further, wherever necessary, the results are obtained using FSDT (eight-noded quadrilateral element with 5 d.o.f. per node, u_0, v_0, w_0, θ_x, θ_y) for comparison purpose. The material properties used, unless otherwise specified, are

$$\textit{Material } 1: E_1/E_2 = 10,\ G_{12}/E_2 = G_{13}/E_2 = G_{23}/E_2 = 0.5,\ v_{12} = v_{23} = v_{13} = 0.25,$$
$$E_2 = 24.2307 \text{ GPa},\ \rho = 2768 \text{ kg/m}^3.$$

$$\textit{Material } 2: E_1/E_2 = 40,\ G_{12}/E_2 = G_{13}/E_2 = 0.6,\ G_{23}/E_2 = 0.5,\ v_{12} = v_{23} = v_{13} = 0.25,$$
$$\alpha_2/\alpha_1 = 1125,\ E_2 = 10^9 \text{ N/m}^2,\ \alpha_1 = 10^{-5}/^{\circ}\text{C},\ \rho = 1500 \text{ kg/m}^3,$$

where E, G, v and ρ are Young's modulus, shear modulus, Poisson's ratio and density. Subscripts 1, 2 and 3 refer to the principal material directions. All the layers are of equal thickness and the ply angle is measured with respect to the x-axis (meridional axis). The spatial distributions of loading considered here are

for thermal case: $\Delta T = T_0\ (2z/h) \sin(\pi x/L) \cos(6\pi y/C)$,
for internal pressure loading case: $q = q_0 \sin(\pi x/L) \cos(6\pi y/C)$.

The analysis of oval cylindrical shell can be studied considering four different classes of spatially fixed asymmetric modes (SS, SA, AS, AA), depending on whether they are symmetric (S) or antisymmetric (A) at the semi-major ($y = 0$ or $C/2$), and the semi-minor ($y = C/4$ or $3C/4$) axes. C is the total circumferential length of the shell. The details of boundary conditions for one-eighth of the shell are:

simply supported edges:

$$v_0 = w_0 = \theta_y = w_1 = \beta_y = \Gamma = \phi_y = \psi_y = 0 \quad \text{at } x = 0, L,$$

along the lines of symmetry:

$$u_0 = \theta_x = \beta_x = \phi_x = \psi_x = 0 \quad \text{at } x = L/2,$$
$$v_0 = \theta_y = \beta_y = \phi_y = \psi_y = 0 \quad \text{at } y = 0, C/4,$$

along the lines of antisymmetry:

$$u_0 = w_0 = \theta_x = w_1 = \beta_x = \Gamma = \phi_x = \psi_x = 0 \quad \text{at } y = 0, C/4.$$

Based on progressive mesh refinement, a 16×8 grid mesh (circumferential and meridional directions) is found to be adequate to model the one-eighth of the shells (quarter in cross-section and half in length) for the present analysis. Before proceeding to the detailed study, the present formulation is tested considering problems for which solutions are available in the literature. Table 1 shows the comparison of present results for thin composite oval shells with the analytical

Table 1
Comparison of non-dimensional frequencies $\Omega[=\omega R_o(\rho/E_1)^{1/2}]$ for a two-layered cross-ply thin oval shell ($R_o/h = 100$, $L/R_o = 1$, $\xi = 0.2$, axial half-wave number $m = 1$, Material 1)

Circum wave no. $\bar{n}$	SS and SA modes			AA and AS modes		
	Ref. [8]	Ref. [12]	Present[a]	Ref. [8]	Ref. [12]	Present[a]
1	0.47023	0.47072	0.47038	0.41044	0.41044	0.41077
2	0.28660	0.28375	0.28324	0.29195	0.29195	0.29240
3	0.20680	0.20729	0.20674	0.20557	0.20557	0.20607
4	0.15844	0.15872	0.15799	0.15825	0.15825	0.15890
5	0.13000	0.13095	0.12987	0.12998	0.12998	0.13093
6	0.10950	0.11055	0.10934	0.10949	0.10949	0.11055
7	0.10865	0.10986	0.10834	0.10864	0.10864	0.10985
8	0.12365	0.12516	0.12332	0.12364	0.12364	0.12516
9	0.13905	0.14059	0.13861	0.13905	0.13905	0.14059
10	0.16227	0.16363	0.16175	0.16227	0.16227	0.16363
11	0.19099	0.19207	0.19043	0.19099	0.19099	0.19207
12	0.22400	0.22469	0.22343	0.22400	0.22400	0.22470

[a] FSDT and HSDT.

Table 2
Comparison of non-dimensional frequencies $\Omega^2[=\omega^2 R_o^2(1-\nu^2)\rho/E]$ for fairly thick isotropic oval shell ($L/R_o = 6$, $\xi = 1.0$, $m = 1$, $\nu = 0.25$)

R_o/h	Circum. wave no. $\bar{n}$	SS and SA modes				AA and AS modes			
		Ref. [14]		Present		Ref. [14]		Present	
		FSDT[a]	PSDT[b]	FSDT[a]	HSDT[c]	FSDT[a]	PSDT[b]	FSDT[a]	HSDT[c]
13.33	0	0.5068	0.5067	0.50225	0.50224	—	—	—	—
	1	0.1702	0.1702	0.16942	0.16958	0.0931	0.0931	0.09252	0.09264
	2	0.4798	0.4796	0.06656	0.06643	0.1502	0.0808	0.08018	0.07996
	3	0.1597	0.1595	0.15916	0.15897	0.1609	0.1608	0.16056	0.16037
	4	0.2884	0.2779	0.29421	0.29434	0.3028	0.2996	0.30009	0.30023
	5	0.4853	0.4845	0.48591	0.48643	0.4847	0.4839	0.48535	0.48588
40.00	0	0.5067	0.5067	0.50210	0.04734	—	—	—	—
	1	0.1696	0.1696	0.16894	0.15928	0.1178	0.1177	0.11691	0.11019
	2	0.4715	0.4714	0.03339	0.03146	0.1506	0.0595	0.05936	0.05595
	3	0.0588	0.0587	0.05870	0.05531	0.0438	0.0438	0.04380	0.04129
	4	0.1035	0.1035	0.10375	0.09778	0.0959	0.1040	0.10402	0.09804
	5	0.1639	0.1638	0.16342	0.15407	0.1666	0.1665	0.16661	0.15708

[a] First order shear deformation theory (shear correction factor $= \pi^2/12$).
[b] Parabolic shear deformation theory.
[c] Higher order shear deformation theory without zig-zag function.

solution [12] and they match well. Since studies pertaining to thick laminated oval case are not readily available, the solutions of fairly thick isotropic case are compared against those of available analytical work [14] in Table 2. It can be noted here that the present finite element

solutions based on FSDT and HSDT for the thickness parameters considered here are, in general, found to be in good agreement with the available study. However, it is further seen from Table 2 that, for antisymmetric vibration mode corresponding to the circumferential wave number $\bar{n}$ equal to 2, the results shown in Ref. [14] using FSDT differs significantly from those of parabolic model even for thin situation. But the present results based on FSDT model are in very close agreement to that of parabolic model [14]. Furthermore, for the symmetric mode of vibration case, the solution for $\bar{n} = 2$ given in Ref. [14] is very high compared to that of corresponding antisymmetric case, whereas the difference obtained in the present study between symmetric and antisymmetric cases is very less. It can be opined from the available literature that, for circular case, the frequency values corresponding to symmetric and antisymmetric vibration cases are equal, irrespective of circumferential wave number, whereas little difference can be noticed for the non-circular case for the lower wave number (see for instance, Table 1). For thick laminated case, the results evaluated based on HSDT are very close to those of three-dimensional finite element solutions [31] compared to the performance of FSDT model as shown in Table 3.

Next, the effect of ovality parameter (ξ) on symmetry–symmetry (SS) and symmetry–antisymmetry (SA) types of vibration modes is demonstrated in Fig. 2, assuming a two-layered shell ($0^\circ/90^\circ$, $L/R_o = 0.5$; $R_o/h = 5$ and 20). It is observed from this figure that, for the given nominal circumferential wave number $\bar{n}$, the discrepancy between corresponding frequencies

Table 3
Comparison of non-dimensional frequencies $\Omega[= \omega R_o(\rho/E_1)^{1/2}]$ for a two- and eight-layered cross-ply thick oval shells ($R_o/h = 6$, $\xi = 0.8$, $m = 1$, Material 2)

No. of layers	L/R_o	Theory	SS mode			SA mode		
			First	Second	Third	First	Second	Third
Two layer	0.5	FSDT	0.5215	0.5702	0.6730	0.5381	0.6102	0.6707
		HSDT	0.4995	0.5483	0.6483	0.5160	0.5875	0.6583
		3-D FEM[a]	0.4865	0.5390	0.6369	0.5063	0.5772	0.6537
	1	FSDT	0.1976	0.2885	0.4690	0.2285	0.3195	0.3704
		HSDT	0.1940	0.2812	0.4503	0.2239	0.3178	0.3581
		3-D FEM[a]	0.1924	0.2776	0.4416	0.2216	0.3172	0.3521
	6	FSDT	0.0487	0.2083	0.4266	0.0487	0.1194	0.3150
		HSDT	0.0477	0.2005	0.4048	0.0487	0.1160	0.3007
		3D FEM[a]	0.0472	0.1965	0.3951	0.0486	0.1141	0.2939
Eight layer	0.5	FSDT	0.6175	0.6820	0.8087	0.6401	0.7131	0.7373
		HSDT	0.6105	0.6730	0.7977	0.6322	0.7094	0.7271
		3-D FEM[a]	0.6064	0.6686	0.7911	0.6281	0.7077	0.7218
	1	FSDT	0.2639	0.3863	0.5883	0.3100	0.3415	0.4831
		HSDT	0.2609	0.3796	0.5782	0.3054	0.3405	0.4743
		3-D FEM[a]	0.2601	0.3772	0.5727	0.3041	0.3403	0.4705
	6	FSDT	0.0768	0.2896	0.5332	0.0501	0.1788	0.4131
		HSDT	0.0746	0.2826	0.5225	0.0501	0.1742	0.4038
		3D FEM[a]	0.0737	0.2799	0.5164	0.0501	0.1725	0.3996

[a] Using ANSYS-5.6, 1997.

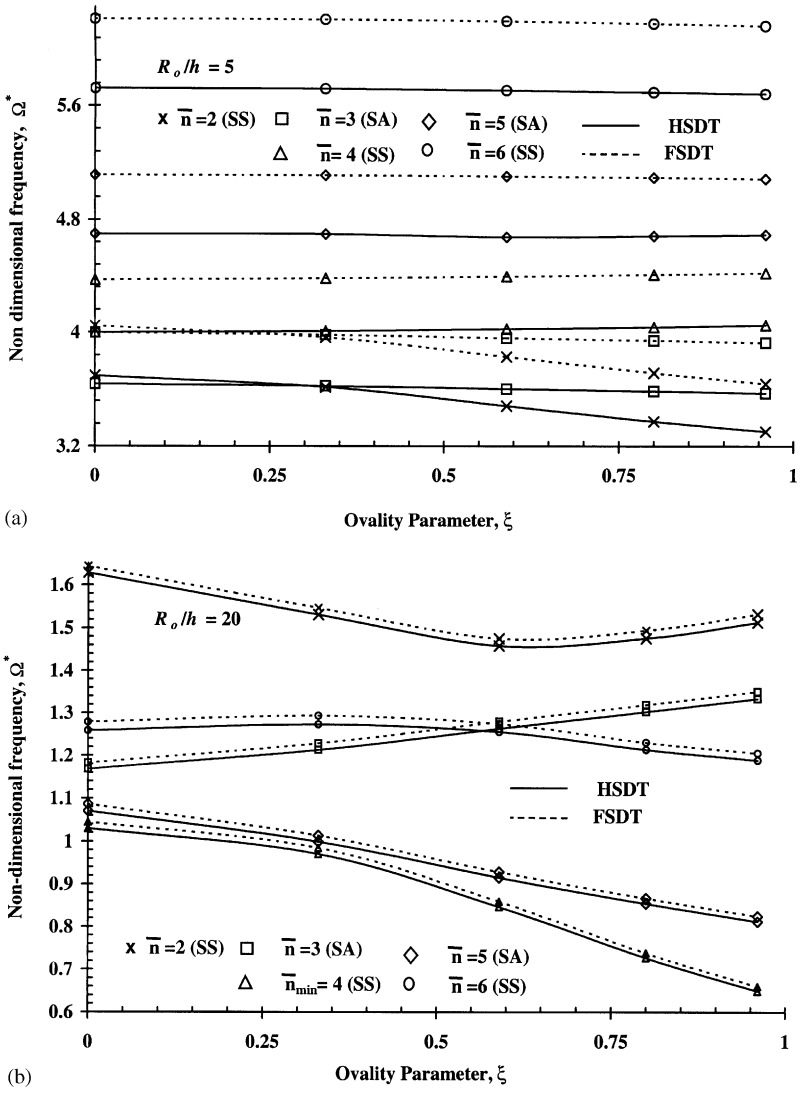

Fig. 2. Non-dimensional frequency versus ovality parameter curves for two-layered cross-ply (0°/90°) oval shell ($L/R_o = 0.5$, $m = 1$, Material 2): (a) $R_o/h = 5$ and (b) $R_o/h = 20$.

($\Omega^* = 12\omega^2 R_o^2(1 - \nu_{13}\nu_{21})\rho/E_1$) based on FSDT and HSDT increases with the increase in the circumferential wave number for the chosen displacement pattern. It is further noticed that, for moderately thin oval shell ($R_o/h = 20$), the circumferential wave number corresponding to the fundamental mode ($\bar{n}_{min}$) is same for all the values of ovality parameter considered here and fundamental frequency value decreases with increase in ovality of the shell. However, for circumferential wave number other than $\bar{n}_{min}$, the variation of frequency value depends on ovality and thickness parameters. This is mainly attributed to the drastic change in the membrane/bending energies of shell with the increase in the non-circularity. It is also seen that, for thick shell

($R_o/h = 5$), the rate of variation of the frequency parameter with ovality parameter is very less with slight decrease/increase for lower/higher modes and the value of $\bar{n}_{min}$ depends on the value of ovality/non-circularity parameter.

The influence of length ratio on the frequency parameters is studied considering SS and SA and AA and AS modes of vibrations of eight-layered thick/thin oval shells ($L/R_o = 0.5$ & 5, $R_o/h = 5$ and 20) and are shown in Tables 4 and 5. It can be opined from these tables that, although, with the increase in the ovality parameter, the wave number corresponding to $\bar{n}_{min}$ remains same, the value of $\bar{n}_{min}$ is different depending on the length parameters. It can be further inferred from these tables that, with increase in ovality parameter, the rate of change in frequency is very less for the higher nominal circumferential wave numbers. This is due to the increase in number of circumferential nodes and, in turn, results in almost constant curvature between the nodes, even though the eccentricity is large. It is seen from these tables that the frequency values, in general, decreases with the increase in the values of non-circular parameter, except for very low nominal circumferential wave number and/or the nominal circumferential wave numbers around the wave number, $\bar{n}_{min}$ corresponding to the lowest frequency values. Such observation can be noticed from the tabulated results pertaining to elliptical shells in Ref. [32]. This is attributed to the geometrical complexities because of ovality, thickness and length ratios. It, in turn, introduces significant variation in the membrane and bending energies for the lower nominal circumferential wave numbers whereas, for higher nominal circumferential wave numbers, it produces predominant changes in the energies due to the coupling of various circumferential modes corresponding to circular one. It can be observed by comparing the results given in these tables with Fig. 2 that the frequency value increases with the increase in number of layers, as expected, due to the weakening of bending–stretching coupling.

The analysis is also carried out to highlight the effect of variation of thickness ratio (R_o/h) on the frequency characteristics of some class of vibration modes (SS and SA), considering a short two-layered oval shell ($0^\circ/90^\circ$, $L/R_o = 0.5$; $\xi = 0.33$ and 0.96). The results are presented in Fig. 3. It is inferred from this figure that, with the increase in the thickness, the frequency parameter value increases for the chosen nominal wave number $\bar{n}$ and the difference between the results obtained using first and higher order models also increases. It is further seen that, for cylinder with low ovality, the value of $\bar{n}_{min}$ varies with respect to thickness parameter, whereas it is same for very thick to fairly thick cases with high ovality.

Finally, the transient dynamic response analysis is conducted considering eight-layered cross-ply thick oval shells [$L/R_o = 1$, $\xi = 0.33$ and 0.96, $h = 0.001$ m, $(0^\circ/90^\circ)_4$] subjected to thermal load ($T_o = 1$). The variations of the transverse (w/h) and in-plane (v/h) displacements with time predicted here are presented in Figs. 4 and 5 for two values of thickness parameter ($R_o/h = 5$ and 10). It is observed from these figures that the maximum amplitude predicted by HSDT model is significantly different from that of FSDT one, and it is even seen for higher thickness ratio case. Furthermore, the transverse displacement obtained using HSDT exhibits high-frequency oscillations because of the participation of thickness stretch modes arising from Γ term in the transverse displacement field. In the case of in-plane displacement, along the circumferential direction, the response characteristics evaluated using HSDT are somewhat qualitatively similar to those of FSDT but the peak amplitudes are different.

Similar studies are conducted for the response characteristics of oval shell subjected to internal pressure ($q_o = 100$). The results obtained for the eight-layered elliptical shells [$L/R_o = 0.5$, $R_o/h =$

Table 4
Non-dimensional frequency parameter $\Omega^*[= 12\omega^2 R_o^2(1-\nu_{13}\nu_{21})\rho/E_1]$ for different nominal circumferential wave numbers of eight-layered cross-ply $(0^\circ/90^\circ)_4$ oval shell ($R_o/h = 5$, $m = 1$, Material 2)

$\bar{n}$	$L/R_o = 0.5$							$L/R_o = 5$						
	Cir. Cyl.	SS and SA modes			AA and AS modes			Cir. Cyl.	SS and SA modes			AA and AS modes		
	$\xi = 0.0$	$\xi = 0.33$	0.59	0.96	0.33	0.59	0.96	$\xi = 0.0$	$\xi = 0.33$	0.59	0.96	0.33	0.59	0.96
1	5.6046	5.8429	6.0163	6.2250	5.4377	5.4283	5.4933	0.0338	0.0390	0.0426	0.0469	0.0286	0.0246	0.0194
2	5.0310	4.9708	4.8638	4.7062	5.0330	5.0374	5.0475	0.0960	0.0942	0.0905	0.0836	0.1015	0.1099	0.1238
3	5.1973	5.1772	5.1517	5.1147	5.1326	4.9783	4.7612	0.4637	0.4566	0.4448	0.4249	0.4537	0.4287	0.3656
4	5.8386	5.8344	5.8259	5.8081	5.8344	5.8258	5.8073	1.1823	1.1688	1.1347	1.0377	1.1697	1.1434	1.0843
5	6.8633	6.8529	6.8306	6.7781	6.8529	6.8306	6.7781	2.2399	2.2251	2.1922	2.1114	2.2250	2.1911	2.1030
6	8.2347	8.2219	8.1940	8.1275	8.2219	8.1940	8.1275	3.6243	3.6084	3.5733	3.4879	3.6083	3.5734	3.4885
7	9.9395	9.9252	9.8944	9.8207	9.9252	9.8944	9.8207	5.3314	5.3147	5.2784	5.1911	5.3147	5.2784	5.1911
8	11.9753	11.9603	11.9278	11.8503	11.9604	11.9277	11.8499	7.3626	7.3455	7.3083	7.2194	7.3455	7.3082	7.2193

Table 5
Non-dimensional frequency parameter $\Omega^*[= 12\omega^2 R_o^2(1-\nu_{13}\nu_{21})\rho/E_1]$ for different nominal circumferential wave numbers of eight-layered cross-ply $(0^\circ/90^\circ)_4$ oval shell ($R_o/h = 20$, $m = 1$, Material 2)

$\bar{n}$	$L/R_o = 0.5$							$L/R_o = 5$						
	Cir. Cyl.	SS and SA modes			AA and AS modes			Cir. Cyl.	SS and SA modes			AA and AS modes		
	$\xi = 0.0$	$\xi = 0.33$	0.59	0.96	0.33	0.59	0.96	$\xi = 0.0$	$\xi = 0.33$	0.59	0.96	0.33	0.59	0.96
1	3.5908	4.1452	4.5727	5.1014	3.1685	3.0414	3.1309	0.0328	0.0381	0.0419	0.0463	0.0272	0.0225	0.0157
2	2.3801	2.3111	2.2499	2.2369	2.4502	2.5587	2.6746	0.0194	0.0181	0.0157	0.0116	0.0194	0.0192	0.0189
3	1.9949	1.9331	1.8528	1.7480	1.9055	1.7399	1.5085	0.0687	0.0676	0.0657	0.0627	0.0674	0.0645	0.0584
4	1.9726	1.9041	1.7467	1.5114	1.9208	1.8456	1.7435	0.2243	0.2217	0.2155	0.1990	0.2218	0.2166	0.2047
5	2.2134	2.2496	2.2998	2.3795	2.2445	2.2607	2.2562	0.5419	0.5317	0.5295	0.5090	0.5379	0.5294	0.5084
6	2.7145	2.7212	2.7637	2.7743	2.7215	2.7432	2.8593	1.0735	1.0680	1.0568	1.0295	1.0680	1.0568	1.0295
7	3.4958	3.4955	3.4950	3.4938	3.4956	3.4949	3.4942	1.8613	1.8546	1.8402	1.8061	1.8546	1.8402	1.8060
8	4.5780	4.5744	4.5666	4.5481	4.5744	4.5665	4.5481	2.9345	2.9265	2.9093	2.8682	2.9265	2.9093	2.8682

5 and 10, $\xi = 0.33$ and 0.96, $(0^\circ/90^\circ)_4$] are described in Figs. 6 and 7. It is observed that the responses predicted using FSDT and HSDT are noticeably different for thick case. However, this difference in the response behavior vanishes with increase in the thickness ratio. The effect of thickness stretching mode, introducing high-frequency oscillation for the transverse motion of shells subjected thermal load, does not affect much the response history of shells under mechanical load.

5. Conclusions

The free vibration characteristics and the transient dynamic response behaviors of laminated cross-ply oval shells are analyzed using higher order displacement model. The effectiveness of the

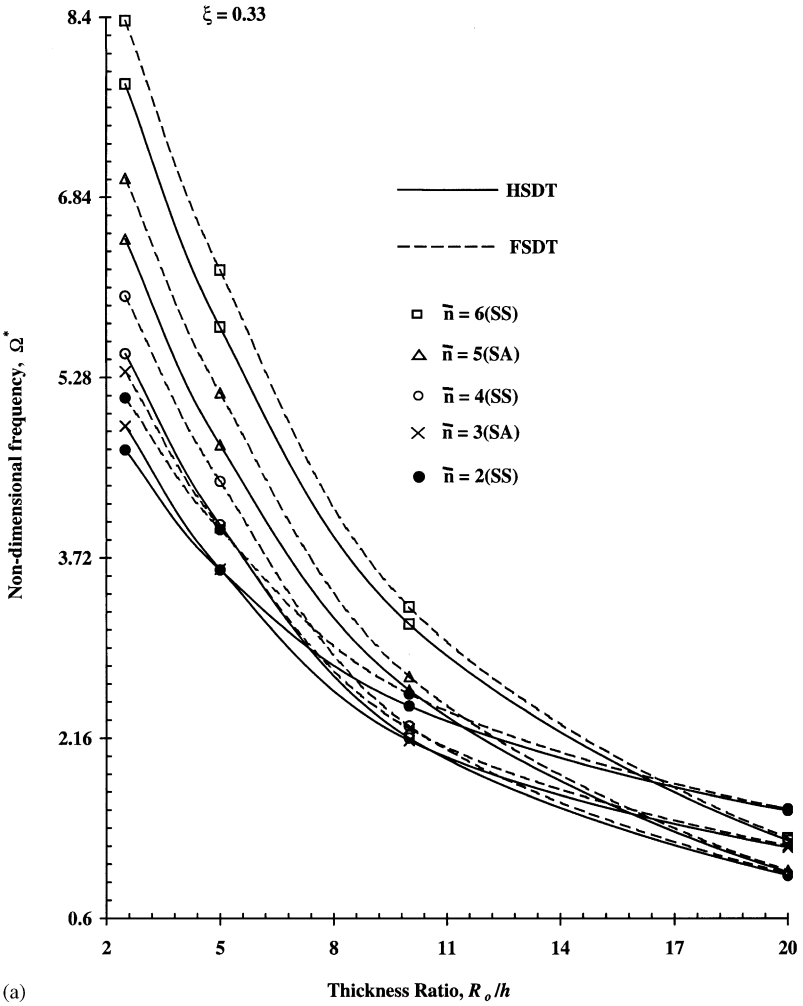

Fig. 3. Non-dimensional frequency versus thickness ratio curves for two-layered cross-ply oval shell with: (a)$\xi = 0.33$ $(0^\circ/90^\circ, L/R_o = 0.5, m = 1$, Material 2) and (b) $\xi = 0.96$ $(0^\circ/90^\circ, L/R_o = 0.5, m = 1$, Material 2).

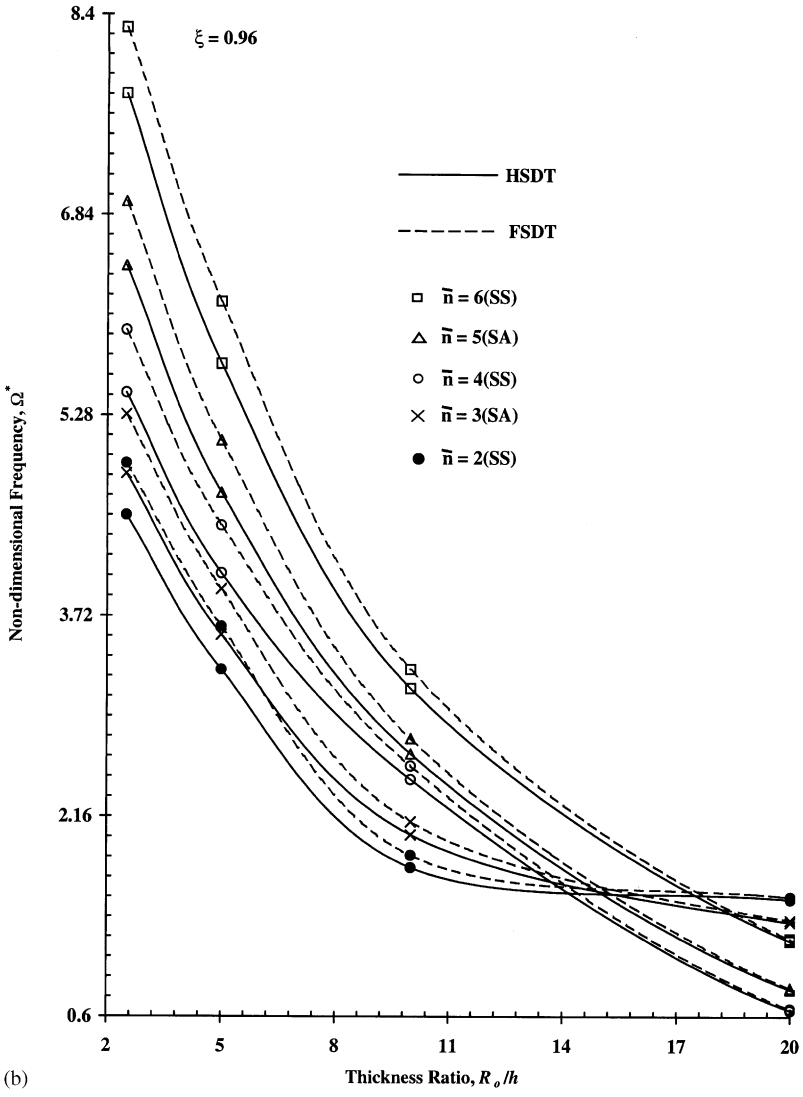

Fig. 3 (*continued*).

present formulation over the first order theory is demonstrated through a parametric study. The following observations can be made from the detailed analysis carried out here:

(i) The variation in the ovality parameter value can significantly alter the frequency values depending on thickness and length ratios, and nominal circumferential wave number.
(ii) The difference between the corresponding frequency values obtained based on FSDT and HSDT increases with the increase in the circumferential wave number and thickness parameter.
(iii) The eccentricity parameter can affect the nominal wave numbers corresponding to the fundamental mode for the two-layered case compared to eight-layered one, depending on thickness value.

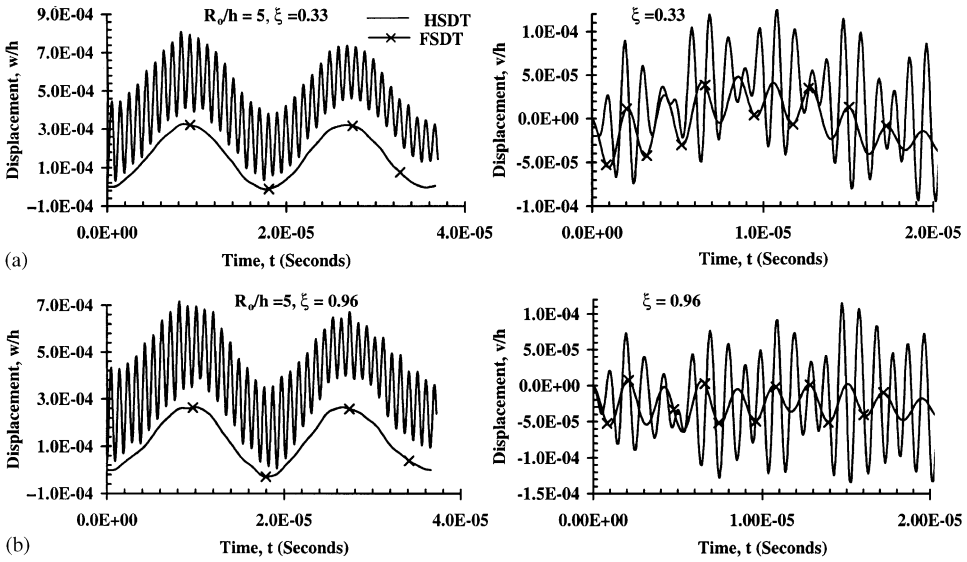

Fig. 4. Response of eight-layered cross-ply $(0^\circ/90^\circ)_4$ oval shell ($R_o/h = 5$, $L/R_o = 1$) subjected to thermal load: (a) $\xi = 0.33$ and (b) $\xi = 0.96$.

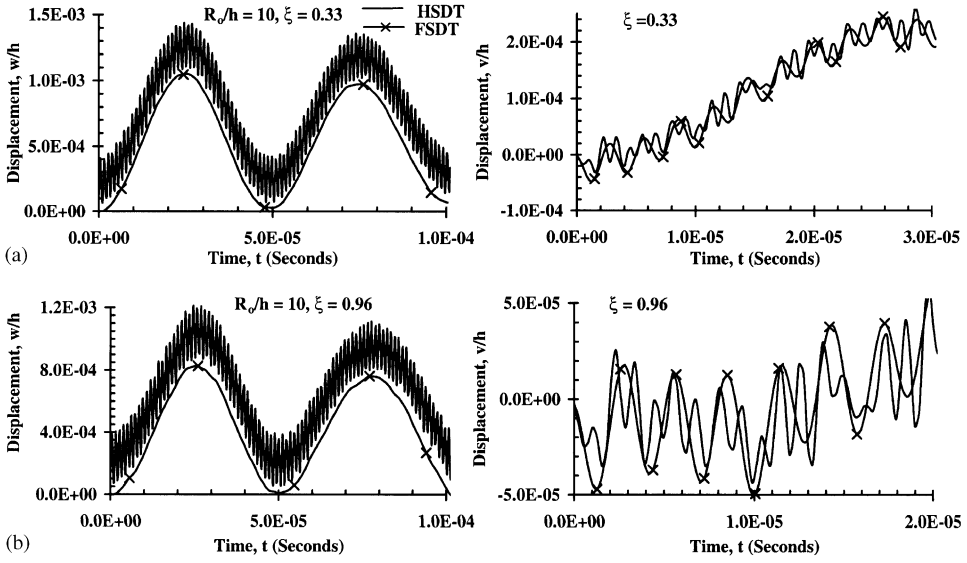

Fig. 5. Response of eight-layered cross-ply $(0^\circ/90^\circ)_4$ oval shell ($R_o/h = 10$, $L/R_o = 1$) subjected to thermal load: (a) $\xi = 0.33$ and (b) $\xi = 0.96$.

(iv) Coupling of circumferential modes, corresponding to circular case, is significant for eccentric shell vibrating at modes with lower nominal circumferential wave numbers.

(v) The participation of high-frequency oscillation in the response history is observed in thermal case.

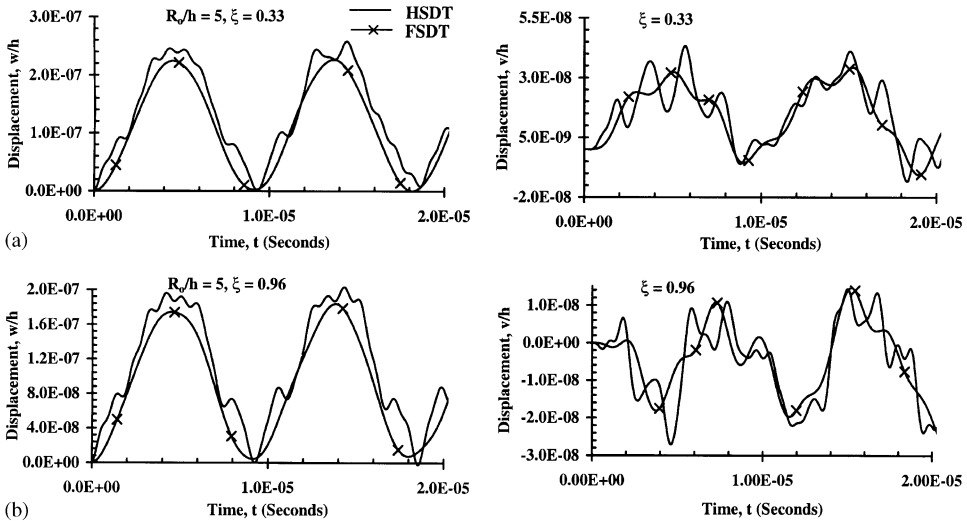

Fig. 6. Response of eight-layered cross-ply $(0^\circ/90^\circ)_4$ oval shell ($R_o/h = 5$, $L/R_o = 0.5$) subjected to pressure load: (a) $\xi = 0.33$ and (b) $\xi = 0.96$.

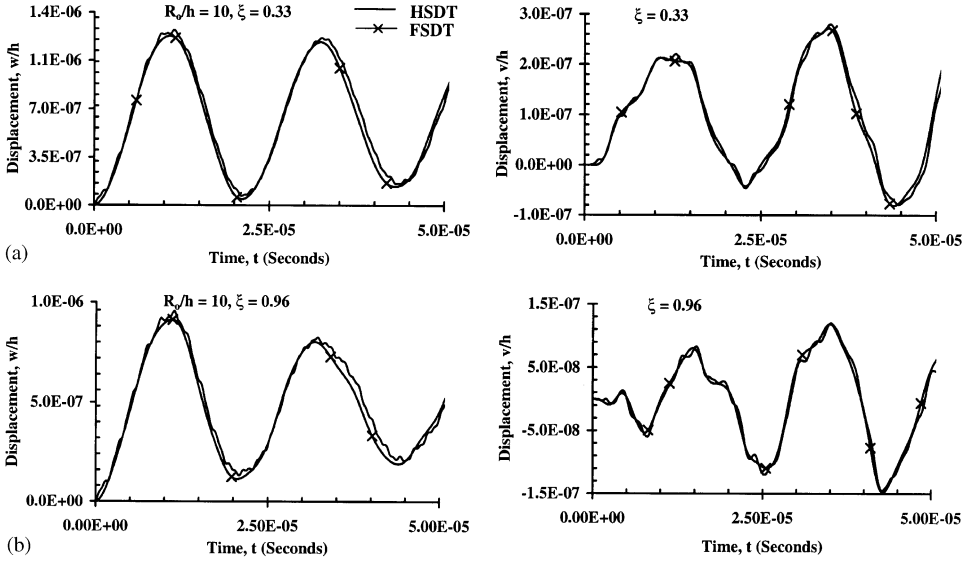

Fig. 7. Response of eight-layered cross-ply $(0^\circ/90^\circ)_4$ oval shell ($R_o/h = 10$, $L/R_o = 0.5$) subjected to pressure load: (a) $\xi = 0.33$ and (b) $\xi = 0.96$.

(vi) The influence of higher order model on the response characteristics of shells subjected to thermal load is considerable, even for fairly thick situation, compared to the mechanical loading case.

Appendix A

The various submatrices involved in Eq. (5b) are

$$[Z_1] = \begin{bmatrix} 1 & 0 & 0 & 0 & 0 \\ 0 & \dfrac{1}{1+z/R} & 0 & 0 & 0 \\ 0 & 0 & 1 & 0 & 0 \\ 0 & 0 & 0 & \dfrac{1}{1+z/R} & 1 \end{bmatrix}, \quad [Z_2] = z[Z_1], \quad [Z_3] = \begin{bmatrix} z^2 & 0 & 0 & 0 \\ 0 & \dfrac{z^2}{1+z/R} & 0 & 0 \\ 0 & 0 & 0 & 0 \\ 0 & 0 & \dfrac{z^2}{1+z/R} & z^2 \end{bmatrix},$$

$$[Z_4] = z[Z_3], \quad [Z_5] = \begin{bmatrix} S^k & 0 & 0 & 0 \\ 0 & \dfrac{S^k}{1+z/R} & 0 & 0 \\ 0 & 0 & 0 & 0 \\ 0 & 0 & \dfrac{S^k}{1+z/R} & S^k \end{bmatrix},$$

$$[Z_6] = \begin{bmatrix} 1 & 0 \\ 0 & 1 \end{bmatrix}, \quad [Z_7] = z[Z_6], \quad [Z_8] = z^2[Z_6],$$

$$[Z_9] = S^k_{,z}[Z_6], \quad [Z_{10}] = \begin{bmatrix} 0 & 0 & 0 & 0 & 0 \\ \dfrac{1}{1+z/R} & \dfrac{z}{1+z/R} & \dfrac{z^2}{1+z/R} & \dfrac{z^3}{1+z/R} & \dfrac{S^k}{1+z/R} \end{bmatrix}, \tag{A.1}$$

$$\{\varepsilon_1\} = \begin{Bmatrix} u_{0,x} \\ v_{0,y} + \dfrac{w_0}{R} \\ w_1 \\ u_{0,y} \\ v_{0,x} \end{Bmatrix}, \quad \{\varepsilon_2\} = \begin{Bmatrix} \theta_{x,x} \\ \theta_{y,y} + \dfrac{w_1}{R} \\ 2\Gamma \\ \theta_{x,y} \\ \theta_{y,x} \end{Bmatrix}, \quad \{\varepsilon_3\} = \begin{Bmatrix} \beta_{x,x} \\ \beta_{y,y} + \dfrac{\Gamma}{R} \\ \beta_{x,y} \\ \beta_{y,x} \end{Bmatrix},$$

$$\{\varepsilon_4\} = \begin{Bmatrix} \phi_{x,x} \\ \phi_{y,y} \\ \phi_{x,y} \\ \phi_{y,x} \end{Bmatrix}, \quad \{\varepsilon_5\} = \begin{Bmatrix} \psi_{x,x} \\ \psi_{y,y} \\ \psi_{x,y} \\ \psi_{y,x} \end{Bmatrix}, \tag{A.2}$$

$$\{\varepsilon_6\} = \begin{Bmatrix} \theta_x + w_{0,x} \\ \theta_y \end{Bmatrix}, \quad \{\varepsilon_7\} = \begin{Bmatrix} 2\beta_x + w_{1,x} \\ 2\beta_y \end{Bmatrix},$$

$$\{\varepsilon_8\} = \begin{Bmatrix} 3\phi_x + \Gamma_{,x} \\ 3\phi_y \end{Bmatrix}, \quad \{\varepsilon_9\} = \begin{Bmatrix} \psi_x \\ \psi_y \end{Bmatrix}, \quad \{\varepsilon_{10}\} = \begin{Bmatrix} w_{0,y} - \dfrac{v_0}{R} \\ w_{1,y} - \dfrac{\theta_y}{R} \\ \Gamma_{,y} - \dfrac{\beta_y}{R} \\ -\dfrac{\phi_y}{R} \\ -\dfrac{\psi_y}{R} \end{Bmatrix}. \tag{A.3}$$

O_1 and O_2 are null matrices of size 4×2 and 4×5, respectively.

Appendix B. Nomenclature

B	strain–displacement matrix
C	total circumferential length
$\dot{d}^e$	vector of the time derivatives of displacement field variables
E_1, E_2, E_3	Young's modulii
F_M, F_T	global mechanical and thermal load vectors
F_M^e, F_T^e	element level mechanical and thermal load vectors
G_{12}, G_{23}, G_{13}	shear modulii
h	total thickness of the shell
h_k, h_{k+1}	z co-ordinates of the inner and outer surfaces of the kth layer
H	interpolation matrix
k	layer number
K, M	global stiffness and mass matrices
K^e, M^e	element level stiffness and mass matrices
L	meridional/axial length of the shell
m	axial/meridional half-wave number
$\bar{n}$	nominal circumferential wave number
$\bar{n}_{min}$	nominal circumferential wave number corresponding to fundamental frequency
N	number of layers
O_1, O_2	null-matrices
q	distributed force acting on the bottom surface of the shell
q_o	amplitude of distributed mechanical load
Q_k	constitutive matrix of kth layer referred to the material principal directions
$\bar{Q}_k$	constitutive matrix of kth layer referred to the laminated shell axes
R	principal radius of curvature in the circumferential direction

R_o	average radius of curvature of the middle-surface
S^k	zig-zag function
t	time
t_k	thickness of kth layer
T	kinetic energy
T_o	amplitude of temperature rise
u^k, v^k, w^k	displacements of kth layer along axial, circumferential and thickness directions, respectively.
u_0, v_0, w_0	reference surface displacements
U_T	total potential energy
w_1, Γ	higher order terms associated with displacement w^k
x	axial/meridional co-ordinate
y	circumferential co-ordinate
z	thickness/radial co-ordinate
z_k	local transverse co-ordinate with its origin at the center of the kth layer
Z	matrix realting the velocity components of a generic point with time derivative of d^e
$\bar{Z}$	matrix relating the middle-surface strains with the strain at any point z
$Z_i\,(i = 1, \ldots, 10)$	sub-matrices of $\bar{Z}$ matrix
$\alpha_1, \alpha_{2,}\alpha_3$	thermal coefficients in the material principal directions
$\alpha_x, \alpha_y, \alpha_z, \alpha_{xy}$	thermal expansion coefficients in the shell co-ordinates
β_x, ϕ_x	higher order terms associated with displacement u^k
β_y, ϕ_y	higher order terms associated with displacement v^k
δ	vector of the degrees of freedom/generalized co-ordinates
δ^e	vector of the elemental degrees of freedom/generalized co-ordinates, and
$\delta_i\,(i = 1, \ldots, n)$	degrees of freedom/generalized co-ordinates
ΔT	rise in temperature
ε	total strain
ε_{bm}	bending and membrane strains
$\varepsilon_i (i = 1, \ldots, 10)$	middle-surface strain vectors
ε_s	transverse shear strains
$\bar{\varepsilon}_t$	thermal strain vector
$\varepsilon_{xx}, \varepsilon_{yy}, \varepsilon_{zz}$	normal strain components
$\left.\begin{matrix}\bar{\varepsilon}_{xx}, \bar{\varepsilon}_{yy}, \bar{\varepsilon}_{zz},\\ \bar{\varepsilon}_{xy}, \bar{\varepsilon}_{xz}, \bar{\varepsilon}_{yz}\end{matrix}\right\}$	components of thermal strain vector $\bar{\varepsilon}_t$
$\gamma_{xy}, \gamma_{xz}, \gamma_{yz}$	shear strain components
$\nu_{12}, \nu_{23}, \nu_{13}$	Poisson ratios
θ_x, θ_y	rotations of the normal to the middle-surface about the y- and x-axis, respectively
ρ_k	mass density of the kth layer
σ	stress vector
ω	frequency
$\Omega, \Omega^2, \Omega^*$	non-dimensional frequency parameters

ξ	non-circularity/ovality parameter
ψ_x, ψ_y	generalized variables associated with the zig-zag function, S^k
$(^\circ)$	partial derivative with respect to time
$()_{,x}$	partial derivative with respect to x
$()_{,y}$	partial derivative with respect to y

References

[1] A.W. Leissa, Vibration of Shells, NASA SP-288, 1973.
[2] A.K. Noor, Bibliography of monographs and surveys on shells, Applied Mechanics Review 43 (1990) 223–234.
[3] A.K. Noor, W.S. Burton, Assessment of computational models for multilayered composite shells, Applied Mechanics Review 43 (1990) 67–97.
[4] M.S. Qatu, Review of shallow shell vibration research, Shock Vibration Digest 24 (1992) 3–15.
[5] K.P. Soldatos, Review of three-dimensional dynamic analysis of circular cylinders and cylindrical shells, Applied Mechanics Review 47 (1994) 501–516.
[6] K.P. Soldatos, Mechanics of cylindrical shells with non-circular cross section: a survey, Applied Mechanics Review 52 (1999) 237–274.
[7] K.P. Soldatos, G.J. Tzivanidis, Buckling and vibration of cross-ply laminated non-circular cylindrical shells, Journal of Sound and Vibration 82 (1982) 425–434.
[8] K.P. Soldatos, A Flugge-type theory for the analysis of anisotropic laminated non-circular cylindrical shells, International Journal of Solids and Structures 20 (1984) 107–120.
[9] D. Hui, H.Y. Du, Effects of axial imperfections on vibrations of anti-symmetric cross-ply, oval cylindrical shells, Journal of Applied Mechanics 53 (1986) 675–680.
[10] K. Suzuki, G. Shikanai, A.W. Leissa, Free vibrations of laminated composite thin non-circular cylindrical shell, Journal of Applied Mechanics 61 (1994) 861–871.
[11] A.K. Noor, Noncircular cylinder vibration by multilocal method, Engineering Mechanics Division, Proceedings of American Society of Civil Engineers 99 (1973) 389–407.
[12] V. Kumar, A.V. Singh, Vibrations of composite noncircular cylindrical shells, Journal of Vibration and Acoustics 117 (1995) 471–476.
[13] K. Suzuki, G. Shikanai, A.W. Leissa, Free vibrations of laminated composite thick noncircular cylindrical shell, International Journal of Solids and Structures 33 (1996) 4079–4100.
[14] K.P. Soldatos, On thickness shear deformation theories for the dynamic analysis of non-circular cylindrical shells, International Journal of Solids and Structures 22 (1986) 625–641.
[15] Y.K. Cheung, C.Z. Yuan, Z.J. Xiong, Transient response of cylindrical shells with arbitrary shaped sections, Thin-Walled Structures 11 (1991) 305–318.
[16] N.D. Phan, J.N. Reddy, Analysis of laminated composite plates using a higher order shear deformable theory, International Journal of Numerical Methods in Engineering 45 (1984) 745–752.
[17] T. Kant, Mallikarjuna, A higher-order theory for free vibration of unsymmetrically laminated composite and sandwich plates-finite element evaluation, Computers & Structures 32 (1989) 1125–1132.
[18] A. Bhimaraddi, A higher-order theory for free vibration analysis of circular cylindrical shells, International Journal of Solids and Structures 20 (1984) 623–630.
[19] K. Bhaskar, T.K. Varadan, A higher-order theory for bending analysis of laminated shells of revolution, Computers & Structures 40 (1991) 815–819.
[20] M. Di Sciuva, U. Icardi, Discrete-layer models for multilayered anisotropic shells accounting for the interlayers continuity conditions, Mechanica 28 (1993) 281–291.
[21] L.H. He, Linear theory of laminated shells accounting for continuity of displacement and transverse shear stresses at layer interfaces, International Journal of Solids and Structures 31 (1994) 613–627.
[22] U. Icardi, Cylindrical bending of laminated cylindrical shells using a modified zig-zag theory, Structural Engineering and Mechanics 5 (1998) 497–516.

[23] J.S.M. Ali, K. Bhaskar, T.K. Varadan, A new theory for accurate thermal/mechanical flexural analysis of symmetrically laminated plates, Composite Structures 45 (1999) 227–232.
[24] D.P. Makhecha, B.P. Patel, M. Ganapathi, Dynamic analysis of laminated composite plates subjected to thermal/mechanical loads using an accurate theory, Composite Structures 51 (2001) 221–236.
[25] H. Murakami, Laminated composite plate theory with improved in-plane responses, American Society of Mechanical Engineers Journal of Applied Mechanics 53 (1986) 661–666.
[26] R.M. Jones, Mechanics of Composite Materials, McGraw-Hill, New York, 1975.
[27] O.C. Zienkiewicz, Finite Element Methods in Engineering Science, McGraw-Hill, London, 1971.
[28] G. Pratap, A C^o continuos 4-noded cylindrical shell element, Computers & Structures 21 (1985) 995–999.
[29] M. Ganapathi, D.P. Makhecha, Free vibration analysis of multi-layered composite laminates based on an accurate higher-order theory, Composite Part B: Engineering 32 (2001) 535–543.
[30] L.D. Culberson, D.E. Boyd, Free vibrations of freely supported oval cylinders, American Institute of Aeronautics and Astronautics Journal 9 (1971) 1474–1480.
[31] ANSYS 5.6 User's Manual, Swanson Analysis Systems Inc., Canonsburg, PA, 1997.
[32] J.L. Sewall, W.M. Thompson, C.G. Pusey, An experimental and analytical vibration study of elliptical cylindrical shells, NASA TN D—6089, 1971.